

A4

PMO's Research Progress on Space Debris

Chen Zhang

Purple Mountain Observatory, Chinese Academy of Sciences

In recent years, Chinese aerospace industry has been greatly developed, and the amount of aerospace activities has rapidly increased to the third all over the world. Meanwhile, China also has responsibilities and obligations to contribute in global space debris work, in order to make the earth orbit resources develop reasonably and peacefully together.

Space debris division of Purple Mountain Observatory, CAS, is the largest and most historical space debris research institute in China, which has been engaged in the researches of Earth orbital artificial spacecraft since the launch of the first man-made satellite, 1957. Till now, it has formed a complete research system, which covers the research areas of Earth orbital dynamics, space debris observation, space situational awareness, collision avoidance, reentry prediction, etc. At the same time, this division operates the largest civilian space situational observation network which consists of dozens of dedicated optical telescopes, such as the Optical Telescope Array, and also maintains the most complete space debris catalogue in China.

Nowadays the division is cooperating openly with other agencies around the world and participating in international affairs actively on space debris issues, to make its own contributions to human aerospace causes.



Biography

Zhangchen

Zhangchen is a primary researcher of space debris division of PMO, CAS since 2006, who respectively studied at NJU, UCAS and USTC. His interests are mainly focused on space debris optical observation related methods and techniques, especially on image reduction, space debris photometry, survey strategies and automated telescope control system. He works as primary staff in several large programs such as Optical Telescope Array, Quad-Channel Telescope construction, space debris physical characteristics research with photometry and spectrometry observation, and he leads some individual researches like spacecraft optical stealth strategy, SSA using astronomical transient survey data and automated transient survey pipeline construction.



PMO's Research Progress on Space Debris

Purple Mountain Observatory, CAS
Key Laboratory of Space Object and Debris Observation

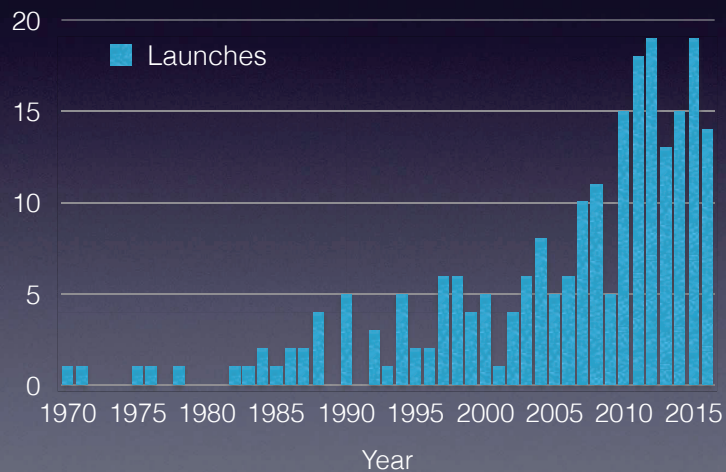
Zhang Chen*, Zhao Changyin
2016/10/18 @ JAXA

Outline

- **Overview of CNSA progress**
- Observation
- Application
- Dynamics

Overview

Successful launches from 1970 to 2016



Mitigation

Jan, 2015-Dec, 2015

19 Launches completed, 45 Payloads.

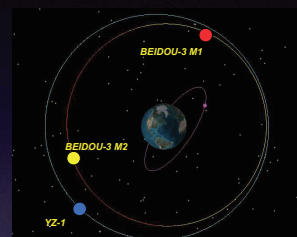
2 in IGSO, 2 in MEO, 5 in GTO, 36 in SSO.

YZ-1 Upper Stage

- Long duration in orbit
- Multiple start
- Deorbit
- Passivation

LM-6 and LM-11

- New generation small launchers
- Orbital stage
- Passivation design



Mitigation

ADR Technology Research

- Space robotic arm
- Space debris detection and identification system based on visual technology
- Space robotic arm movement planning algorithm and control
- Ground test
- Flight demonstration

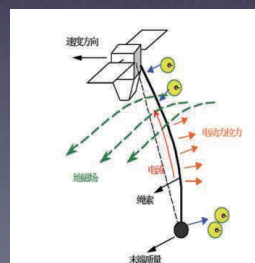
Electrodynamic Tether

EDT deorbiting strategy

Initial ejection phase: uncontrolled Tether

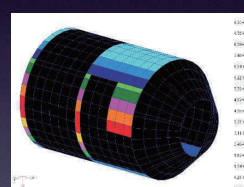
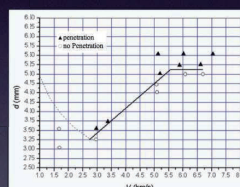
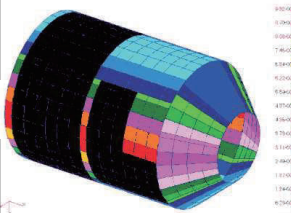
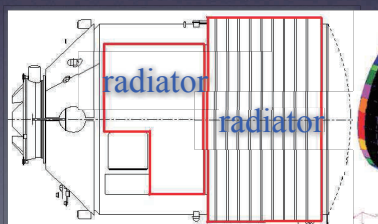
Active releasing phase: Kissel control law

Deorbiting phase: Current on/off control to maintain the stability of the Tether

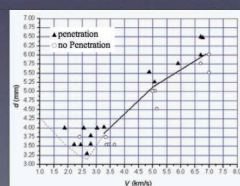


Tiangong Protection

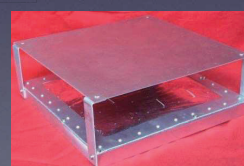
- Shield Tiangong-1 was launched on September 29 2011, On-orbit performance is healthy and the protection design was verified through this typical flight.
- Radiator and its support panel taken as Whipple Protection
- PNP: 0.13 before, 0.37 after
- Cone face/Side face protected by bumper (Whipple)
- PNP: 0.37 before, 0.70 after



Whipple with standoff 51mm normal impact

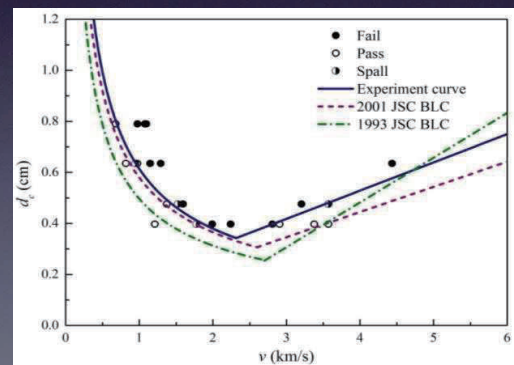
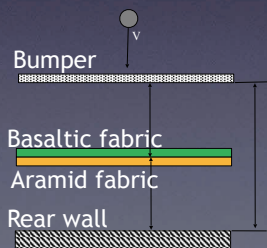
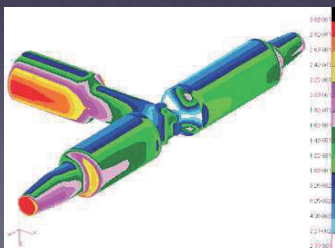


Whipple with standoff 70mm normal impact



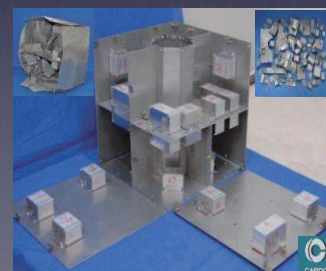
Space Station Protection

- $PNP=0.0$, if no shielding; $PNP=0.3$, if Whipple
- Advanced shield and advanced materials
- Critical parameters of shield have been determined
- $PNP=0.92$, if Stuffed Whipple



Protection Research

- Database for HVI data and engineering application
- The damage of satellite's Remote Terminal Unit (RTU) under hypervelocity impact has been studied. The work of redundancy design has been accomplished for RTU
- Satellite Breakup Model in CARDC (China Aerodynamics Research and Development Center) has been studied
- Satellite Fragmentation Analysis (SFA) has been developed



Observation and Collision Avoidance

- Routine observation on Chinese non-functional spacecraft and upper stage
 - 100 objects of these kinds in daily observation plan
 - More attention on new launches to support mitigation measures
- International cooperation on observation and re-entry prediction
 - QCT located in Yaoan and some other tracking facilities participate the IADC AI 31.2 campaign 2 times
 - From 2011 to 2015, China has taken part in IADC re-entry campaign 7 times and submitted dozens of re-entry prediction results.
- Space debris thumbing research for ADR
 - Theoretical study on long term spin-down and photometric features
 - Survey scheme to filter the candidates for further research

Space Debris Division, PMO

- Originated from first man-made satellite supporting mission, 1957
- Started systematical operation from China's first satellite mission, 1970
- Now, it is the largest civilian space debris research institute whose research field covers observation, application and dynamics of space debris
- 22 research staffs, 26 support staffs, and 5 graduate students.



Outline

- Overview of CNSA progress
- **Observation**
- Application
- Dynamics

Observation

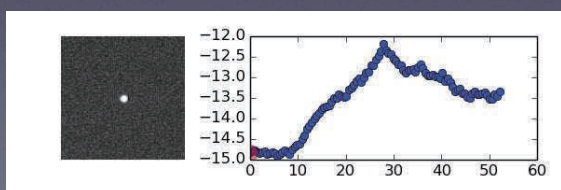
- Operate the largest optical telescope network in China with 7 sites and dozens of dedicated facilities for space debris
- Develop special type of facilities for survey or characteristic research except for the conventional tracking telescopes
- Data center for data collecting, track correlating, orbit determination, prediction and storage
- Improve algorithm of detection, extraction, calibration, image restoration for the optimized observation strategy

Tracking Facilities



Tracking Method

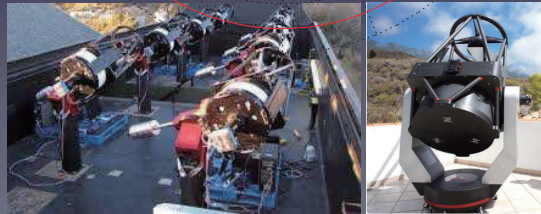
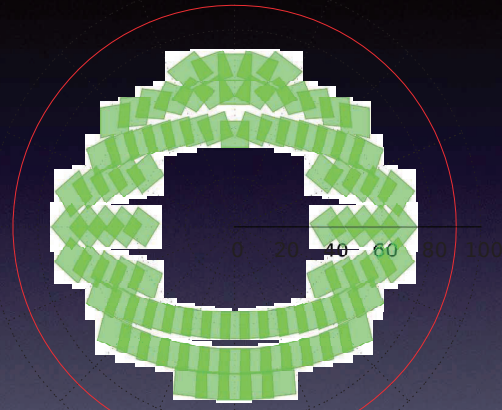
- Moving object detection while in waiting state using morphology
- Close loop speed guidance based on center offset of target
- Fast astrometry and photometry calibration with star prediction
- Object detection technique based on prior information, with high precision and little time cost:
 1. Set a gate around the object image according to prior information;
 2. Obtain the background and RMS value, extract the object pixels;
 3. Decide whether it is a object;
 4. Centering with modified moment in the gate;
 5. Obtain the coordinate on the whole frame



Sun et al. 2013, ChA&A

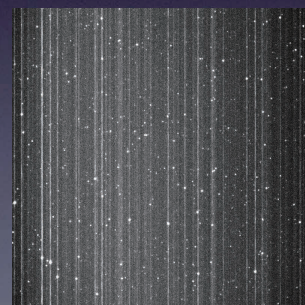
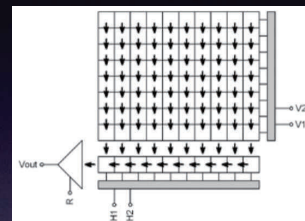
Large Field Telescope Array

- A composite system for space debris survey
- Fixed pointing telescope array covers low altitude ring for fast moving LEO and some of HEO debris
- Motorized telescope array covers high altitude even whole sky for HEO and GEO debris
- Larger follow-up telescope for precise tracking and photometry



Fixed Array Features

- Custom refractor with f-number greater than $f/1$, extreme large FOV
- Background de-smear for full frame ccd without shutter
- GPU-accelerated full field scanning for realtime detection powered by nVidia CUDA tech
- Quasi-realtime object recognition and track correlation for rapid SSA and follow-up observation guidance

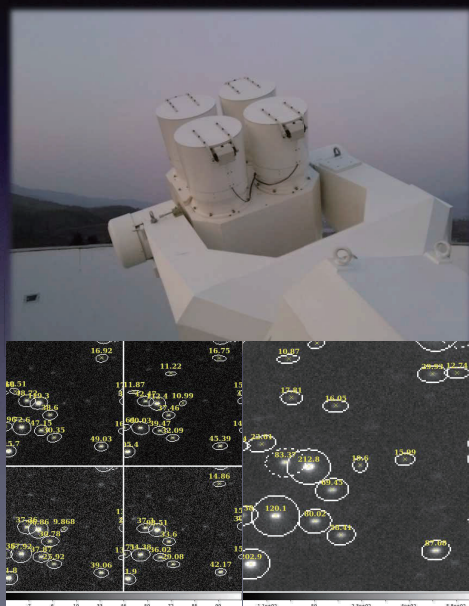


Motorized Array Features

- Optimized survey strategy for improving HEO and GEO detection efficiency
- Fast streak detection and extraction based on differencing and morphology
- Instant guidance and prediction with sparse streaks
- Flexible control for special tasks, such as interception mode or synthetic aperture mode

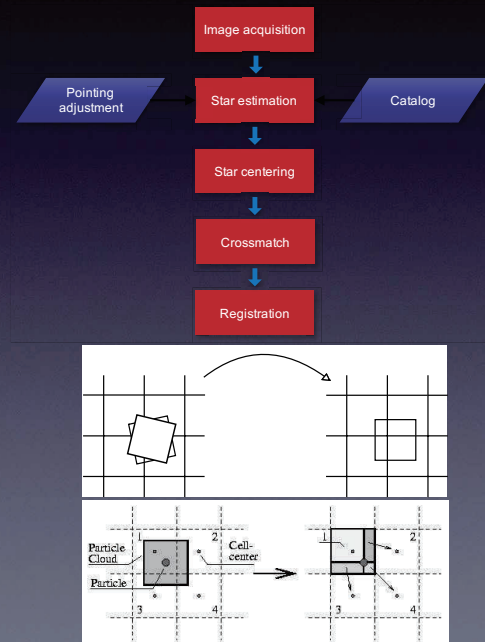
Multi-Channel Telescope

- Synthetic aperture design to gain the profit of both large FOV and deep detection
- Multi-camera synchronized trigger
- Realtime image coadding benefit from fast image registration and CIC reprojection method
- Quad-Channel Telescope as coaxial prototype



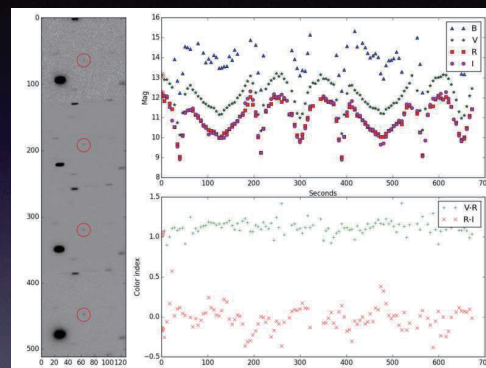
Fast Co-adding

1. Star position estimation using rough pointing information to avoid full frame scanning
2. Image registration in pixel space without blind star cross matching and WCS fitting
3. Cloud in cell algorithm used in cosmology simulation analysis is implemented for fast reprojection
4. Can be extended to motorized array easily



Multi-color Photometry

- To meet the requirement of synchronize multi-color photometry because the debris' luminosity varies rapidly
- Using different filters on QCT's channels
- Do photometry calibration with Landolt catalog to standardize color index
- Automated observation system and pipeline also developed



NORAD 28417U
Indian Com Sat
Defunct
B V R I Band
V-R R-I Index

Observation Methods

Reducing the image degradation

- Separate blended images and handle the smear noises using mathematical morphology transformation (Sun et al. 2014, AJ; Sun et al. 2013, PASJ; Sun et al. 2012, ScChG)
- Image restorations for precise astrometry (Sun & Zhao 2014, RAA)

Object detection and measurement

- Automatic object detection technique for high-Earth orbital space debris survey (Sun et al. 2015, AcAau)
- Adaptive threshold in centering for spinning objects (Sun & Zhao 2014, AdSpR)
- Position estimation based on prior information (Sun et al. 2013, ChA&A)

Source extraction and calibration

- High-precision cross-match algorithm (Sun et al. 2015, AcASn)
- Source extraction method based on mathematical morphology transformation (Sun & Zhao 2012, RAA)
- Reduction pipeline for non-dedicated telescopes (Sun et al. 2016, RAA)

Image Reducing

- According to the relative movements between space object and the background stars in the focal plane, the blending of the images is inevitable.
- The blending of images affects the object detection, and reduces the accuracy of both astrometry and photometry.



- Based on the mathematical morphology transformation, the image blending is addressed, the raw image, 3D-plot, contour plot of the reduction process are presented.
- A set of images simulated with Iraf is adopted to test the precision promotion after de-blending. The results are compared with the ones reduced by SExtractor.

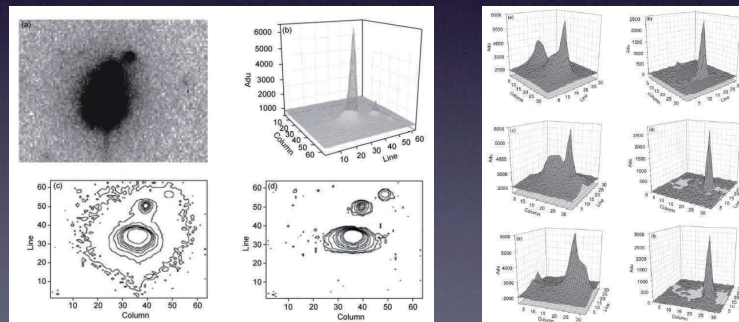
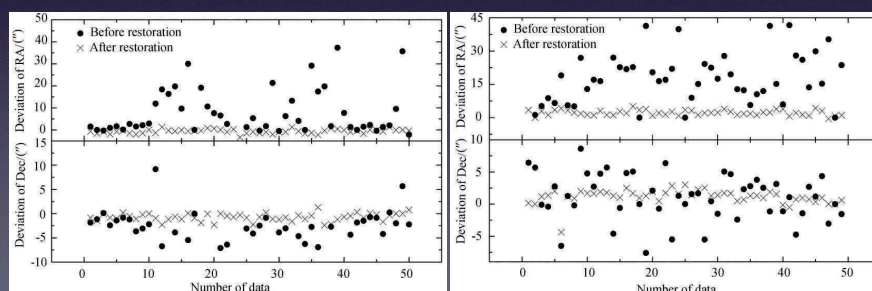


Table 3 Statistical deviation and rms of measured parameters

Coordinate	Measured before separation		Measured after separation		Measured by sextractor	
	Average deviation	RMS	Average deviation	RMS	Average deviation	RMS
X (pixels)	-0.792	2.423	4.425×10^{-2}	0.258	-0.397	2.118
Y (pixels)	-1.132	1.276	-5.659×10^{-2}	0.244	-0.784	1.229

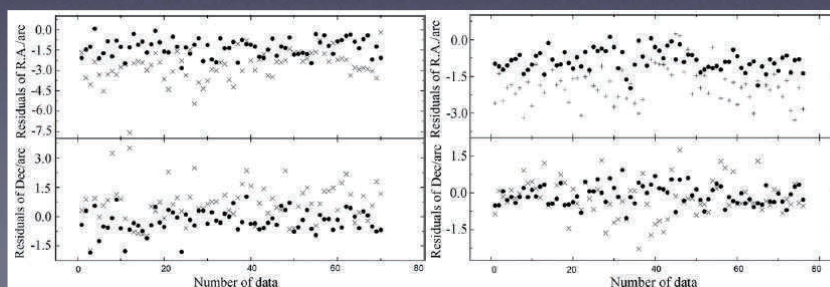
- Various image degradation exists in optical space debris observation, e.g. optical distortion, under-sample and pointing error of the telescope. The reduction accuracy and efficiency are affected.
- Image restoration with the maximum entropy algorithm is adopted to improve the astrometry.



Arc ID	Before restoration			After restoration		
	RMS of RA	RMS of Dec	RMS overall	RMS of RA	RMS of Dec	RMS overall
1	12.91	8.05	15.21	1.14	1.09	1.58
2	24.01	3.88	24.32	2.55	1.60	3.01

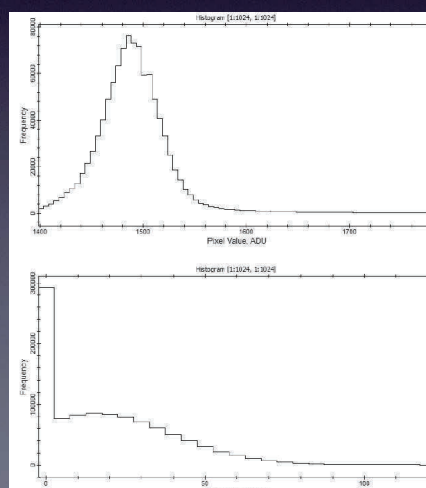
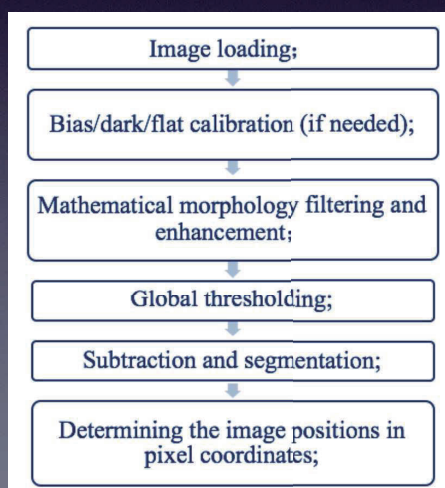
- Image restoration with the mathematical morphology filtering is also performed. The promotion of the measurement accuracy as well as two sample arcs is shown.

Arc ID	Before Transformation			After Transformation		
	rms of R.A. Residuals/Arc	rms of Decl. Residuals/Arc	Overall /Arc	rms of R.A. Residuals/Arc	rms of Decl. Residuals/Arc	Overall /Arc
1	1.78	1.00	2.05	0.97	0.62	1.15
2	1.81	1.03	2.09	0.75	0.61	0.97
3	1.70	1.05	2.00	0.91	0.65	1.12
4	1.75	1.13	2.09	0.85	0.82	1.18
5	1.58	1.06	1.91	0.95	0.72	1.20
6	1.56	0.98	1.85	0.68	0.44	0.82
7	1.66	1.19	2.05	0.74	0.56	0.93
8	1.40	0.86	1.64	0.85	0.54	1.01
9	1.46	0.74	1.64	0.68	0.42	0.80
10	1.75	0.76	1.91	0.81	0.54	0.97
11	1.79	1.16	2.13	0.96	0.99	1.38
12	1.63	0.99	1.91	0.98	0.60	1.15
13	1.76	1.20	2.14	0.91	0.84	1.25
14	1.40	0.89	1.66	0.68	0.68	0.96



Detection

- Source extraction without the prior information.
- The mathematical morphology transformation is adopted as a non-linear high-pass filter, which reduces the noise level. Global threshold can be applied after processing.



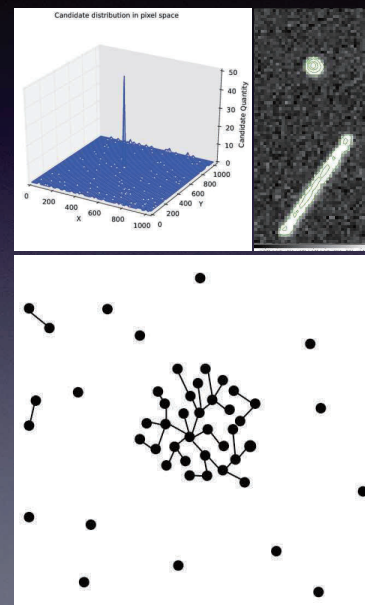
- An automatic object detection algorithm is developed for high-Earth orbital surveys.
- After eliminating the background stellar using the movement information, the detection of GEO object is performed by a simple median; while a two-neighborhood detection algorithm is applied for MEO moving objects.
- Three sets test observations are made, the efficiency is demonstrated compared with the catalogue.

Observation No.	Observation time	Number of theoretical objects	Number of detected objects	Detection ratio
1	1 hour	111	109	98.2%
2	1 hour	122	116	95.1%
3	1 hour	126	119	94.4%

Cluster Identification

- Open loop tracking is widely used in follow-ups to get more stable imaging quality
- An improved post observation pipeline called Cluster Identification is developed, less false alarm, less missing point, more adaptive and no prior knowledge needed

1. Candidate filter using morphology
2. Put all candidates in pixel space
3. Locate dense cluster with FoF algorithm* which is used in halo finder of cosmology simulation
4. Track-let fitting

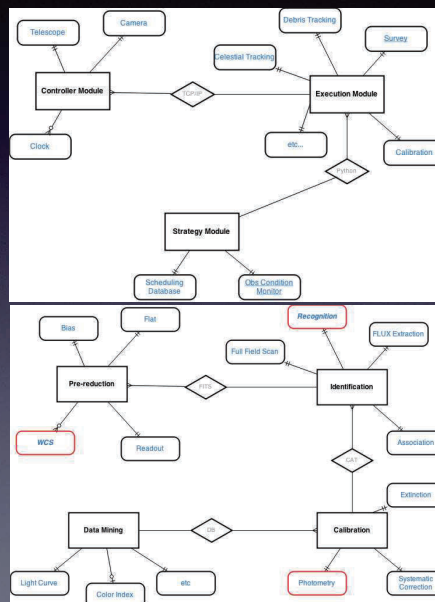


Zhang, and Ping., CAA., 40.3, 399 (2016)

Automated Observation

- Flexible observation system consists of controller and pipeline, for unattended massive follow-ups
- Developed with C / python, driven by database and network, easy for migration and deployment
- Uniform scheduler and HCI, to deeply integrate all telescope resources to maximize observation efficiency

Zhang, master thesis



Outline

- Overview of CNSA progress
- Observation
- **Application**
- Dynamics

Application

- Several kinds of applications are carried out based on the network and massive data
- Traditional orbital cataloging and prediction
- Collision avoidance
- Atmosphere modeling and re-entry prediction
- Photometry and physical characteristics survey

Calculation Method of Collision Probability

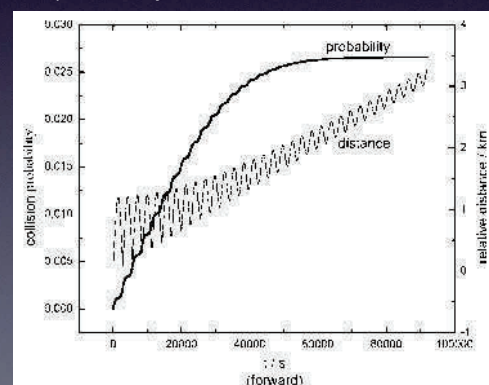
A new method is developed to compute collision probability, to give an explicit expression to compute collision probability which is expressed as a function of the radial and the cross section components of the relative position and error covariance.

The method of calculation of collision probability is developed under the assumption of nonlinear relative motion between two involved space objects.

$$P = P_R \cdot P_T$$

$$= \left\{ \frac{\exp \left[\frac{4(r_a - \Delta h)}{\sqrt{2\pi}\sigma_r} \right]}{1 + \exp \left[\frac{4(r_a - \Delta h)}{\sqrt{2\pi}\sigma_r} \right]} - \frac{\exp \left[\frac{4(-r_a - \Delta h)}{\sqrt{2\pi}\sigma_r} \right]}{1 + \exp \left[\frac{4(-r_a - \Delta h)}{\sqrt{2\pi}\sigma_r} \right]} \right\} \cdot \left\{ \frac{\exp \left[\frac{4(r_t - \rho_{\min})}{\sqrt{2\pi}\sigma_t} \right]}{1 + \exp \left[\frac{4(r_t - \rho_{\min})}{\sqrt{2\pi}\sigma_t} \right]} - \frac{\exp \left[\frac{4(-r_t - \rho_{\min})}{\sqrt{2\pi}\sigma_t} \right]}{1 + \exp \left[\frac{4(-r_t - \rho_{\min})}{\sqrt{2\pi}\sigma_t} \right]} \right\}$$

Catalog Number	TCA (UTC)	Min Range (km)	Position Error (km)	General Method	This Method
25415&31445	Mar 18 14:44:34	0.115	0.128	1.24×10^{-5}	1.52×10^{-5}
20737&20738	Mar 17 10:39:31	0.104	0.380	1.70×10^{-6}	2.15×10^{-6}
27939&31588	Mar 16 13:46:21	0.098	0.073	3.01×10^{-5}	3.51×10^{-5}
11308&32315	Mar 15 03:02:16	0.094	0.107	1.80×10^{-5}	2.05×10^{-5}
17583&37442	Mar 16 14:02:50	0.039	0.011	9.39×10^{-5}	1.88×10^{-4}



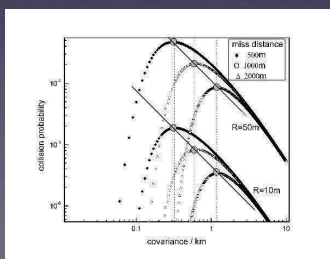
Xu and Xiong, SCIENCE CHINA Physics, 2013

Xu and Xiong, Research in Astronomy and Astrophysics, 2014

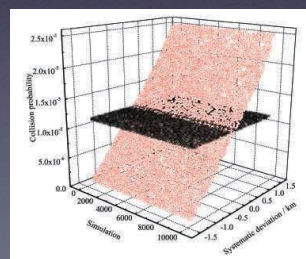
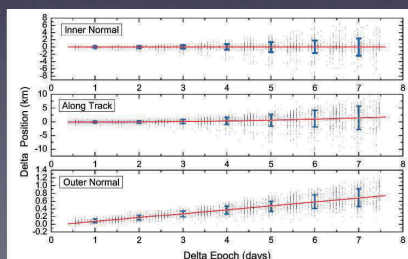
Confidence Level of Collision Probability

The maximum collision probability: with a large positional uncertainty, a Gaussian calculation will produce a low conjunction probability. The resulting probability may give a false sense of confidence that conjunction is not likely to occur. When the covariance data are insufficient or not available, the maximum collision probability is applied.

Discussion of orbital systematic error by data simulation and statistical analysis: A modified formula to calculate collision probability is developed, and the effects of systematic error on the calculation of collision probability are discussed.



Xu, master thesis



Improvement of the Upper Atmosphere Density Model Density Improvement (CHAMP data)

- Nonlinear correction method of atmospheric density for geomagnetic calm and low disturbance is studied.
- Using the data of champ satellite accelerometer, a nonlinear correction function containing 12 coefficients is constructed for the prediction of atmospheric total density over the next few days.

Improvement function:

$$\rho_{\text{true}} = \rho_{\text{model}} + \Delta\rho = \rho_{\text{model}} \left(1 + \frac{\Delta\rho}{\rho_{\text{model}}} \right) = \rho_{\text{model}} (1 + \varepsilon)$$

$$\varepsilon = \varepsilon_1(\varphi) + \varepsilon_2(t) + \varepsilon_3(h) + \varepsilon_4(F_{10.7})$$

$$= c_1 \cos \varphi + c_2 \sin \varphi + c_3 \cos 2\varphi$$

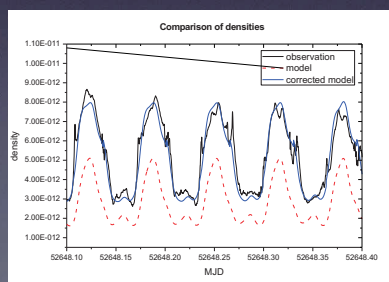
$$+ \delta (c_4 \cos \varphi + c_5 \sin \varphi + c_6 \cos 2\varphi)$$

$$+ (1 - \delta)(c_1 \cos \varphi + c_2 \sin \varphi + c_3 \cos 2\varphi)$$

$$+ c_{10} (h - 400) / 200$$

$$+ c_{11} F_{10.7} / 150$$

$$+ c_{12}$$



Effect of improvement

Improvement of the Upper Atmosphere Density Model Coefficient Improvement (space debris drag data)

- Atmospheric density model correction method for retrieving atmospheric density model parameters from space debris orbit decay data is studied.
- The existing atmospheric density model parameters are improved using dozens of space debris orbit attenuation data to improve the orbit prediction accuracy of space debris.

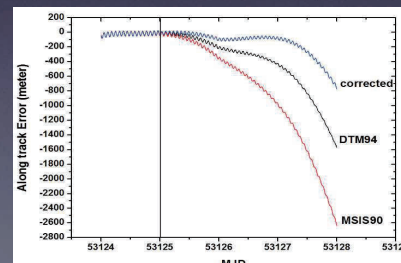
Improvement equation:

$$\rho = 1.6603 \times 10^{-21} \times [4n_{Re}(z) + 16n_D(z) + 28n_{S_2}(z) + 32n_{O_2}(z)]$$

$$n_i(z) = A_i e^{\phi_i(z)} f_i(z)$$

$$\dot{\alpha}_0 - \dot{\alpha}_c = \sum \frac{\partial \dot{\alpha}_c}{\partial \epsilon_i} \Delta \epsilon_i, \epsilon_i \text{ include } A_i \text{ and } AM \text{ etc.}$$

Effect of orbit prediction :
Efficient: ~ 70% case
Inefficient: ~ 30% case



Re-entry Prediction

The work about atmosphere density model was applied to IADC re-entry prediction campaigns, such as UARS and ROSAT etc.

Agency	All Predictions		Last 48h Predictions	
	Count	Error Δt (%)	Count	Error Δt (%)
ASI	24	5.76	11	8.53
BNSC	9	18.89	5	9.18
CNES	12	5.96	4	7.92
CNSA	20	7.35	11	4.85
DLR	16	9.06	7	6.79
ESA	20	8.50	12	7.75
ISRO	28	7.30	13	8.20
JAXA	7	4.28	-	-
NASA	7	6.51	4	6.37
ROSCOSMOS	27	5.54	13	5.30
total	170		80	

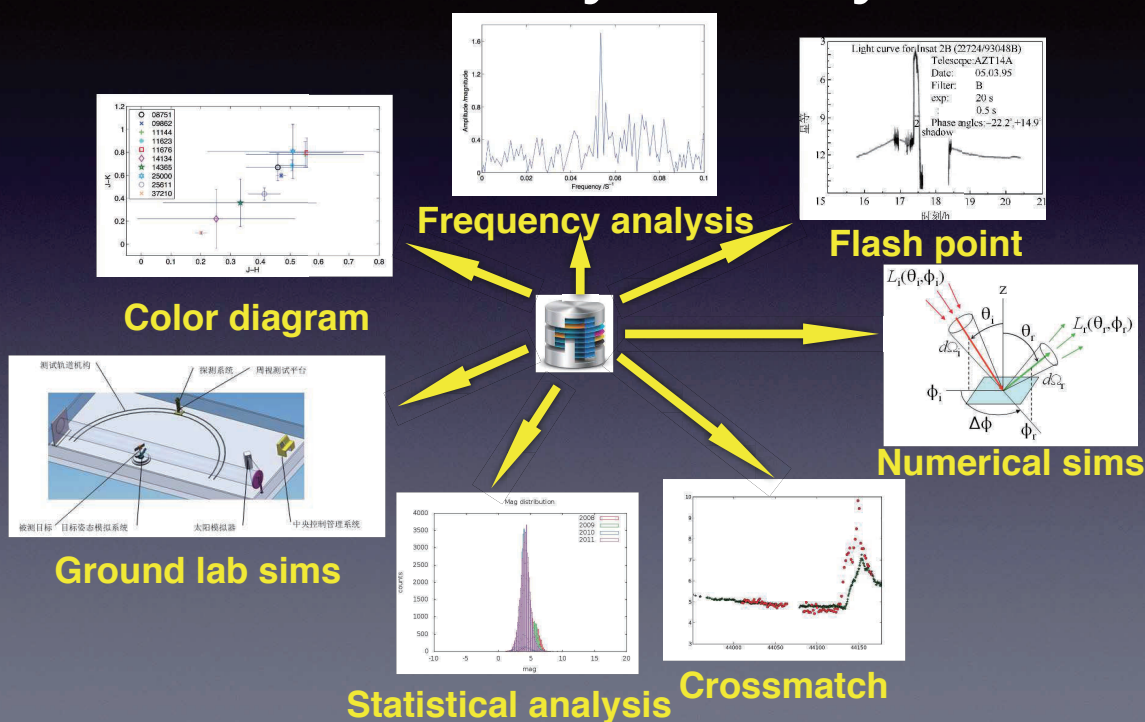
Activities During the Entire Campaign						
P.o.C.		Predictions		TLE Data Access		Osc. Elem. Access
		Inputs	Err (%)	Inputs	Retrievals	Inputs
Pardini	(ASI)	19	19.56	29	0	6
Herridge	(BNSC)	9	13.53	76	0	6
Laporte	(CNES)	7	18.23	2	0	0
Xiong	(CNSA)	11	16.36	2	0	0
Wiedemann	(DLR)	11	28.86	72	0	1
Klinkrad	(ESA)	7	19.48	11	0	2
Ganeshan	(ISRO)	19	15.95	85	0	6
Hirose	(JAXA)	10	19.77	10	0	0
Johnson	(NASA)	9	23.93	17	95	1
Ivanov	(ROSCOSMOS)	24	22.82	88	14	9
		126		392	109	31

Photometry Survey

- Thanks to the modern detector photometry data can be derived while doing astrometry
- Photometry pipelines are developed for different types of telescopes and observation modes
- Photometry is integrated into routine observation and forms a very large photometry database
 - Telescope array provide most of data points (10^8 /yr) as background survey
 - Tracking telescope can provide more complete light curves
- We are trying to open it to the public as a service

Zhang et al.: Space Debris Res. 1, 28 (2013)

Photometry Analysis



Physical Characteristics

- Physical characteristics can be used in target identification, classification and awareness
 1. Optical cross section estimation by magnitude
 2. Attitude and rotation analysis with light curves
 3. Material analysis with color-index
 4. Further more, spectrometry and polarimetry are introduced to extend the knowledge

Outline

- Overview of CNSA progress
- Observation
- Application
- **Dynamics**

Dynamics

- Long history of doing artificial objects dynamics research since the 1970s
- Systematic research on dynamical evolution of GEO
- Long-term orbital dynamical evolution of special orbits such as Molniya
- Rotational motion of space debris

Systematic Research on Dynamical Evolution of GEO

- The dynamics of GEO are complex.
 - **Difficulties:** detection and identification, orbit determination and prediction
- Theoretical investigation on dynamics of GEO is imperfect.
 - **Unsolved problems:** double libration, quantitative variation of inclination, and etc.

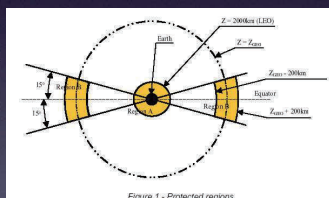
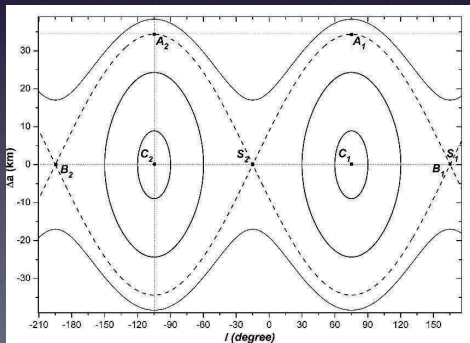
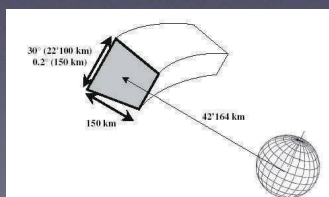


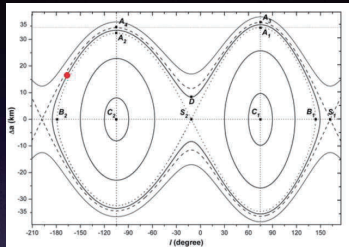
Figure 1 - Protected regions



Four motion patterns:

L1, L2, D1 and D2 ?

Explanation of the Double Libration State in Theory (2D motion: radial and longitudinal directions)



L1,
L2,
L3,
D1
and
D2

Table 1
Equilibrium positions of the space debris orbiting the geosynchronous ring.^a $a_s = 42164.2$ km $a_c = a_s + 2.1 = 42166.3$ km.

	Libration centers c_1 and c_2		Saddle points s_1 and s_2	
	l_{c_1} (degree)	l_{c_2} (degree)	l_{s_1} (degree)	l_{s_2} (degree)
I	75.07	-104.93	165.07	-14.93
II	73.86	-103.70	165.55	-15.43
III	75.06	-104.91	162.05	-11.34
IV	74.98	-104.19		

Table 2
Main characteristic parameters of the 2D phase plane structure.

	The maximum libration half widths or amplitude $(\Delta a)_{max}$ (km)					Boundary values of l (degree)	
	Simple libration		Double libration			l_{B_1}	l_{B_2}
	Δa_{A_1}	Δa_{A_2}	Δa_{A_3}	Δa_{A_4}	Δa_D		
I	34.4	34.4				165.07	-194.93
III	34.5	32.4	36.4	34.4	11.6	143.74	-178.94
IV	34.5	32.3	36.4	34.4	11.6		

Main characteristic parameters in the 2D phase plane (including equilibrium points and their stability, the maximum libration half width and the libration period) determine the variation ranges of the semi-major axis a and longitude l .

Libration period: T_{c_1} : 745 - 1385 days; T_{c_2} : 918 - 1593 days (simple libration)

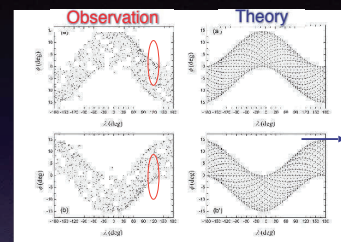
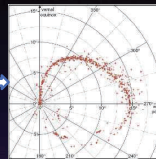
Zhao et al.: Adv. Space Res. 52, 677 (2013) T_D : 2962 - 3232 days (double libration)

Quantitative Variation of Inclination (3D: + Inclination)

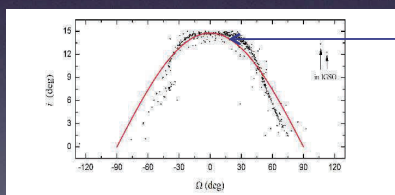
$$\Delta i = \begin{cases} [i_* - 2\alpha, i_*] & (i_* \geq 2\alpha), \\ [2\alpha - i_*, i_*] & (\alpha \leq i_* \leq 2\alpha), \\ [i_*, 2\alpha - i_*] & (i_* \leq \alpha). \end{cases} \quad \alpha \approx 7.4^\circ$$

$$\sin^2(i_* - \alpha) = (\sin \Omega_0 \sin i_0)^2 \frac{\eta}{\eta - \xi} + (\sin \alpha \cos i_0 - \cos \alpha \cos \Omega_0 \sin i_0)^2$$

Derived the analytical expression of the variation range of the orbital inclination



limit the search areas



$$\cos \Omega = \cot \alpha \tan \frac{i}{2} \quad (\alpha \approx 7.4^\circ)$$

The analytical expression for the statistic distribution characteristic of space debris in the orbital plane

the correlation between ϕ and λ

$$\tan \phi = \tan i \sin(\lambda + \theta_G - \Omega)$$

The distribution characteristic of geographic latitude and longitude

Explained the phenomenon that the variation range of the orbital inclination of geostationary orbit is stabilized within about 15 degrees in theory

Application of Theoretical Results

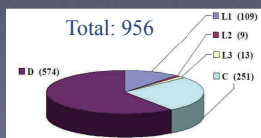
- Proposed a method by using only one set of known orbital elements to determine the motion state and the variation ranges of motion parameters (uncontrolled)

- Motion states: five patterns (L1, L2, L3, D1 and D2)
- Motion parameters: in orbital plane + 2D phase plane (3D: a, i, i)

Motion state	L1	L2	L3	D1	D2
Fitting result	104	42	12	141	424
Theoretical result	97	35	3	140	422

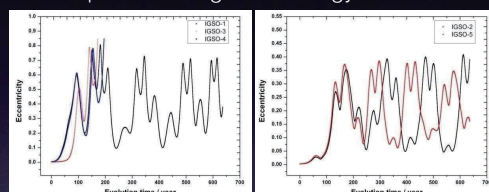
- Theoretical results are consistent with fitting results except in the case of the libration period for some individual space debris that closely approach the separatrices in the 2D phase plane.
- Motion parameters in the states of D1 and D2: (always neglected in the past)

Based on observation data, the classification database for GEO objects is established.

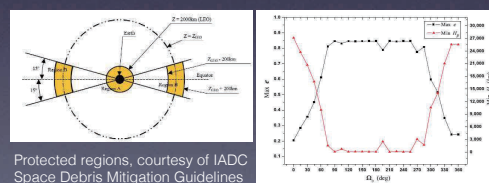


Zhao et al.: *Astrophys. Space Sci.* 361, 196 (2016)

- A new possible mitigation strategy for IGSO



The variation of the eccentricities of IGSO satellites will not always remain small after a long time evolution and can reach to high values.



Protected regions, courtesy of IADC Space Debris Mitigation Guidelines

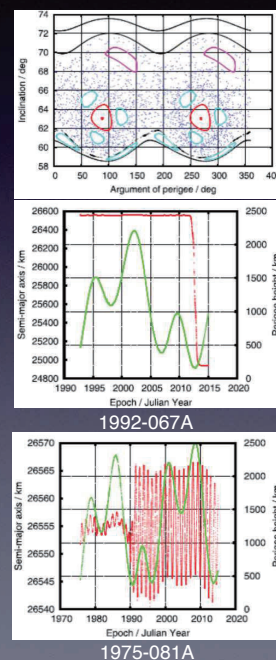
By choosing an appropriate launch time (i.e. the initial longitude of ascending node), the orbital lifetime of the IGSO satellite with high inclination can be reduced significantly.

Research on Dynamical Evolution of Molniya-type Orbits

- Constructed a two-degree-of-freedom Hamiltonian system of Molniya-type orbits under the effect of geopotential, presented the analytic solution, libration width and centre period for the intermediate period motion with a time scale of several years, and explained the amplitude variation of semi-major axis.
- Derived another first integral of the two-degree-of-freedom Hamiltonian system analytically with the Von-Zeipel transformation.
- Established a double resonance model with three periodic terms of luni-solar perturbations, presented the long time-span phase space structure of Molniya-type orbits via Poincaré surface of section and the quantitative results of the period of argument of perigee for typical orbits, and interpreted the chaotic motion using the resonance overlap criterion.

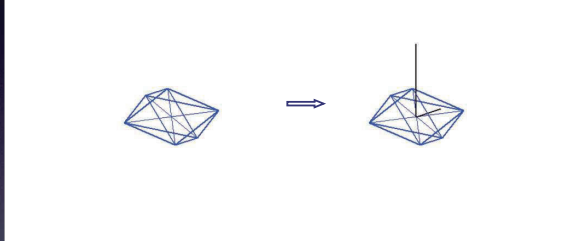
Zhu et al.: *Adv. Space Res.* 54, 197 (2014)

Zhu et al.: *Astrophys. Space Sci.* 357, 126 (2015)



Research on Rotational Motion of Space Debris

A method that using light intensity data to estimate the rotational states



	Expressions	Numerical results	Theoretical value	Error
f_s	Mean value	$3.28958 \times 10^{-3}/s$	$3.28966 \times 10^{-3}/s$	<0.1%
	Frequency	$1.187 \times 10^{-6}/s$	$1.188 \times 10^{-6}/s$	0.1%
	Amplitude	$6.61 \times 10^{-7}/s$	$6.62 \times 10^{-7}/s$	0.2%
	Phase	3.41 rad	3.41 rad	0.6%
f_B	Mean value	$2.32997 \times 10^{-3}/s$	$2.32992 \times 10^{-3}/s$	<0.1%
	Frequency	$1.186 \times 10^{-6}/s$	$1.188 \times 10^{-6}/s$	0.2%
	Amplitude	$4.52 \times 10^{-7}/s$	$4.50 \times 10^{-7}/s$	0.4%
	Phase	0.30 rad	3.41 rad	0.9%

estimate rotational state

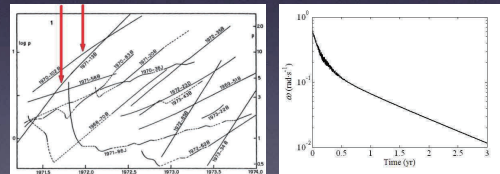
	Estimation results	Preset value	Error
ψ_{j0}	193.2°	191.6°	1.6°
θ_{j0}	43.3°	44.1°	0.8°
θ_0	49.6°	49.7°	0.1°
A/C	3.1681	3.1667	<0.1%
ω	3.2020×10^{-2} rad/s	3.2017×10^{-2} rad/s	<0.1%

The expression and long-term effect of eddy current torque

$$M_E = B \times (L \cdot (\omega \times B))$$

$$L = \begin{pmatrix} M_1 & -M_4 & -M_5 \\ -M_4 & M_2 & -M_6 \\ -M_5 & -M_6 & M_3 \end{pmatrix}$$

Explained the observed phenomenon of change in the spin decay rate in the historical data through numerical simulation.




Found the self-spin of space debris resonates with the orbital motion ultimately; the angular momentum also gradually tends toward the normal of the orbital plane.

Lin et al.: Adv. Space Res. 57, 1189 (2016)

Lin & Zhao.: Astrophys. Space Sci. 357, 167 (2015)

Contacts

- Zhang Chen zhangchen@pmo.ac.cn
- Zhao Changyin cyzhao@pmo.ac.cn
- Xiong Jianning xjn@pmo.ac.cn
- Sun Rongyu rysun@pmo.ac.cn
- Xu Xiaoli xlxu@pmo.ac.cn
- Zhang Mingling mjzhang@pmo.ac.cn
- Zhu Tinglei zhutinglei@pmo.ac.cn
- Lin Houyuan linhouyuan@pmo.ac.cn



Thank you!!